

Quantum statistical forces via reservoir engineering

Shanon L. Vuglar,^{1,2} Dmitry V. Zhdanov,³ Renan Cabrera,² Tamar Seideman,³ Christopher Jarzynski,⁴ Herschel A. Rabitz,² and Denys I. Bondar²

¹University of Melbourne, Parkville, VIC 3010, Australia

²Princeton University, Princeton, NJ 08544, USA

³Northwestern University, Evanston, IL 60208, USA

⁴University of Maryland, College Park, MD, 20742, USA

(Dated: November 10, 2016)

We show that, as in classical statistical physics, the effect of a dissipative environment on a quantum probe can be described by a quantum statistical force. Using Operational Dynamic Modeling, an environment is designed to exert a desired quantum statistical force on a quantum probe. In particular, we simulate an environment tailored to enhance quantum tunneling. We also provide a possible experimental implementation for this environment. These findings highlight the flexibility offered by non-equilibrium open quantum dynamics.

PACS numbers: 03.65.Ta, 03.65.Ca, 03.63.Yz

Introduction. Within classical statistical mechanics, a dissipative environment exerts a statistical force (also known as a fluctuation induced force [1] or entropic force [2]) on a probe immersed in that environment. However, these forces are generally nonadditive [3] and non-universal, explicitly depending on previous dynamics [1]. The aim of this Letter is to extend the concept of statistical forces to the domain of quantum mechanics and to exploit it to enhance desired quantum dynamical properties of systems of interest.

It is widely believed that coupling a quantum system to a bath inevitably destroys its unique quantum dynamical features. However, quantum reservoir engineering [4–10], whereby a bath is designed to enhance a desired dynamical property of a quantum system, has shown that it is possible to preserve and even enhance quantum dynamical features of a system through judiciously coupling the system to a dissipative environment. Proposed applications of quantum reservoir engineering include amplification [11], nonreciprocal photon transmission [12], photon blockade [13], efficient photoinduced charge separation in solar energy conversion [14], implementation of quantum gates [15], and generation entangled quantum states [16–21], squeezed states [22–24], and other interesting quantum states [25–28].

In this Letter, we show how reservoir engineering can be used to implement a quantum statistical force that enhances a desired quantum dynamical property. We illustrate our approach with the hallmark quantum mechanical phenomenon of tunneling, where a potential barrier exerts a repulsive force on an approaching particle. According to widespread belief, interaction with a dissipative bath destroys the coherence of the quantum particle thereby suppressing tunneling rates [29]. However, decoherence-enhanced tunneling was recently experimentally demonstrated in lithium niobate [30]. This is pos-

sible because lithium niobate lacks inversion symmetry, whereas, in GaAs under similar experimental conditions [31], the combination of inversion symmetry and fast interband decoherence results in a negligible tunneling rate. Inspired by this result, we show that there exists a class of environments which significantly enhance tunneling rates, and provide a numerical simulation that illustrates our finding. This effect is not simply due to thermal excitation; these environments exert a quantum statistical force on the particle, which opposes the force exerted by the potential barrier. We give a physical interpretation in which the environment is implemented by collisional dynamics.

General Formulation. Statistical forces are effective forces that can be used to describe the statistical tendency of a macroscopic system to evolve towards states with greater entropy [32]. For example, consider a polymer that has many possible configurations of equal energy. If such a polymer is immersed in a heat bath, then it will tend to arrange itself into configurations that maximize its entropy.

Consider a probe with coordinate x and momentum p in a potential $U(x)$ that exerts a force $F_{pot}(x)$ on the probe:

$$F_{pot}(x) = -\frac{dU(x)}{dx}.$$

Suppose that the environment exerts a statistical force $F_{ent}(x)$ on a probe that depends on the temperature T and entropy $S(x)$ of the environment:

$$F_{ent}(x) = T \frac{dS(x)}{dx}.$$

Then the dynamics of the probe will satisfy the following equations, known as Ehrenfest relations, where $\langle \cdot \rangle$

denotes expectation with respect to a *classical* ensemble:

$$\frac{d}{dt}\langle x \rangle = \frac{1}{m}\langle p \rangle, \quad (1)$$

$$\frac{d}{dt}\langle p \rangle = -\left\langle \frac{dU(x)}{dx} \right\rangle + \left\langle T \frac{dS(x)}{dx} \right\rangle. \quad (2)$$

Here, Eq. (1) relates the velocity and momentum of the probe, and Eq. (2) arises from the balance of forces acting on the probe.

We now consider a quantum probe, and apply Operational Dynamical Modeling (ODM) [33, 34] to show how a given quantum statistical force $F_{ent}(x)$ can be implemented via a dissipative environment. In particular, we derive an expression for a class of environments, described in terms of Lindblad dissipators, which result in the desired quantum statistical force. For a discussion of environments that lead to translationally invariant statistical forces $F_{ent}(p)$ that are functions of the probe's momentum, see Ref. [34]. To apply ODM, we require Ehrenfest relations that the system should satisfy. Motivated by the classical case, Eqs. (1) and (2) are assumed to also apply to a quantum probe, where $\langle \cdot \rangle$ now denotes the expectation with respect to a *quantum* ensemble.

The subsequent derivations employ the phase space formulation of quantum mechanics [35–37], where the Wigner function $W = W(x, p)$ is a real valued function of coordinate x and momentum p that describes the state of the quantum system, the expectation value of an observable O is defined by

$$\langle O \rangle = \int O(x, p) W(x, p) dx dp,$$

and the evolution of a quantum system coupled to a dissipative environment is described as follows:

$$\frac{d}{dt}W = -\frac{i}{\hbar}(H \star W - W \star H) + \sum_{k=1}^{k_{\max}} \mathcal{D}_{A_k}[W], \quad (3)$$

$$H = \frac{1}{2m}p^2 + U(x), \quad (4)$$

$$\mathcal{D}_A[W] = \frac{1}{\hbar} \left(A \star W \star A^* - \frac{1}{2} W \star A^* \star A - \frac{1}{2} A^* \star A \star W \right). \quad (5)$$

The Lindblad dissipators \mathcal{D}_A describe the couplings between the system and the environment. Finally, the binary operator \star is the Moyal product [35–37]

$$\star := \exp \frac{i\hbar}{2} \left(\overleftarrow{\partial}_x \overrightarrow{\partial}_p - \overleftarrow{\partial}_p \overrightarrow{\partial}_x \right), \quad (6)$$

where $\overleftarrow{\partial}_{x,p}$ and $\overrightarrow{\partial}_{x,p}$ denote partial derivatives acting to the left and right respectively: $f \overleftarrow{\partial}_{x,p} g = g \partial_{x,p} f$, $f \overrightarrow{\partial}_{x,p} g = f \partial_{x,p} g$.

To satisfy Eqs. (1) and (2), $A = A(x, p)$ must solve the following equations:

$$\sum_k A_k^* \star \frac{\partial A_k}{\partial p} - \frac{\partial A_k^*}{\partial p} \star A_k = 0, \quad (7)$$

$$\sum_k A_k^* \star \frac{\partial A_k}{\partial x} - \frac{\partial A_k^*}{\partial x} \star A_k = -2iT \frac{dS(x)}{dx}. \quad (8)$$

These equations admit the following general solution, obtained using the methodology of Ref. [34]:

$$\begin{aligned} A_k(x, p) &= \tilde{R}_k(x) \left[1 + i\mathcal{K}_{F_k, \tilde{R}_k}(x) \right] \\ &= R_k(x) e^{i\mathcal{K}_{F_k, R_k}(x)}, \end{aligned} \quad (9)$$

$$\mathcal{K}_{F, R}(x) = \int \frac{F(x)}{R^2(x)} dx. \quad (10)$$

Here $\tilde{R}_k(x)$, $R_k(x)$ and $F_k(x)$ denote arbitrary real valued functions subject to the constraint

$$\sum_k F_k(x) = T \frac{dS(x)}{dx}. \quad (11)$$

Note that $\tilde{R}_k(x)$ and $R_k(x)$ are related to each other as $R_k(x) = \tilde{R}_k(x) \sqrt{1 + \mathcal{K}_{F_k, \tilde{R}_k}(x)^2}$.

Equation (9) defines the class of Lindblad dissipators $A(x, p)$ that satisfy the Ehrenfest relations (1) and (2), and result in a quantum statistical force $F_{ent}(x)$ exerted on the probe. Note that Eq. (9) is in phase space, however, $A(x, p)$ turns out to not depend on p .

We now apply this result to quantum tunneling. Suppose we wish to engineer an environment which enhances quantum tunneling rates by exerting a statistical force that opposes the force a potential barrier exerts on a probe, i.e. $\left\langle T \frac{dS(x)}{dx} \right\rangle = \left\langle \frac{dU(x)}{dx} \right\rangle$. This can be achieved by specializing the constraint (11) as

$$\sum_k F_k(x) = \frac{dU(x)}{dx}. \quad (12)$$

For A_k as in Eqs. (9) and (12), the expected momentum $\langle p \rangle$ of the probe will remain constant as it approaches the potential barrier, significantly enhancing tunneling rates.

Physical Interpretation. We now provide a possible physical implementation of the dissipator in Eq. (3) with $k_{\max} = 2$. Assume that the quantum probe is an atom of mass m in the non-degenerate ground electronic state, with electric polarizability α , and negligible magnetic polarizability. We will consider the motion of the probe along the \vec{e}_x -axis through the effective barrier $U(x) = -\alpha \mathcal{E}(x)^2/4$, created by the off-resonant, blue-detuned (i.e. $\alpha < 0$) laser field $\vec{e}_x \mathcal{E}(x) \cos(\omega(t - z/c))$.

In the presence of an additional, static magnetic field of the form $\vec{e}_z \mathcal{B}(x)$, the statistical force for “bulldozing” the barrier $U(x)$ can be created by two counterpropagating

electron jets, in which the electrons have opposite magnetic moments $\hat{\mu}_s = \pm \hat{\sigma}_z \mu_B$, incident velocities $\pm \vec{e}_x \frac{p_0}{m_e}$, and fluxes $\pm \vec{e}_x j$ (here μ_B is Bohr magneton). The probe is then subject to effective pressure caused by electron recoils. In the absence of a magnetic field, the mean impacts of both jets mutually compensate each other. However, the opposite electron spin polarizations of the jets break this symmetry (and hence, create a nonzero net force on the probe) when a magnetic field is applied. To quantitatively describe this effect, we assume that i) the electron flux j is low enough to neglect multiple scattering of electrons, ii) all interactions of electrons with the probe can be modeled as ideal elastic backscattering events, and iii) the incident electron velocity $\frac{p_0}{m_e}$ is much larger than the characteristic velocities of the probe and

$$p_0 \gg \sqrt{2\mu_B m_e |\mathcal{B}(x)|}. \quad (13)$$

This inequality allows the wavefunctions of incident electrons in the jets to be modeled semiclassically as

$$\psi_{\pm} \propto \frac{e^{\frac{\pm i}{\hbar} \int \tilde{p}_{\pm}(x) dx}}{\tilde{p}_{\pm}(x)}, \quad \tilde{p}_{\pm}(x) = \sqrt{p_0^2 \pm 2\mu_B m_e \mathcal{B}(x)}. \quad (14)$$

The effect of the jets on the probe can then be described by the dissipator $\mathcal{D}_{A+} + \mathcal{D}_{A-}$ [as in Eq. (3)] with

$$A_{\pm} = C e^{\frac{\pm 2i}{\hbar} \int \tilde{p}_{\pm}(x) dx}, \quad C = \sqrt{\hbar \tilde{\sigma} j}, \quad (15)$$

where $\tilde{\sigma}$ is the scattering cross section. Here C^2/\hbar is a coupling constant describing the collective effect of the electron jets on the probe, whereas the exponent in Eq. (15) describes the effect of the individual electrons. Since Eq. (15) is of the form (9), we can immediately identify the bulldozing condition from (12):

$$2\tilde{\sigma} j (\tilde{p}_+ - \tilde{p}_-) = \frac{dU(x)}{dx}. \quad (16)$$

Equation (12) admits the following solution:

$$\mathcal{B}(x) = \frac{\hbar}{16\mu_B m_e C^4} \frac{dU(x)}{dx} \sqrt{16p_0^2 C^4 - \left(\hbar \frac{dU(x)}{dx}\right)^2}. \quad (17)$$

A detailed microscopic theory behind the Lindblad terms (15) will be the subject of a subsequent work.

Simulation. Using the split operator approach proposed in Ref. [38], numerical solutions were obtained for Eq. (3) with $k_{\max} = 2$, A_{\pm} as given in Eq. (15), $\tilde{p}_{\pm}(x)$ as given in Eq. (14), $\mathcal{B}(x)$ as given in Eq. (17), and $m = 1837$ a.u. (the mass of the Hydrogen atom); atomic units (a.u.), $\hbar = m_e = 2\mu_B = 1$, are used throughout.

Figures 1, 2, and 3 show simulation results for the Wigner function of a Gaussian wavepacket

$$W(x, p) = N \exp\left(\frac{-(x - x_0)^2}{2\sigma_x^2} - \frac{(p - p_0)^2}{2\sigma_p^2}\right) \quad (18)$$

moving towards a Gaussian potential barrier

$$U(x) = 2K_0 \exp\left(\frac{-x^2}{2}\right), \quad (19)$$

where N is a normalization constant and K_0 is the initial kinetic energy of the wavepacket $W(x, p)$. Note that since we model quantum tunneling, it is important that the height of the potential barrier in Eq. (19) exceed the initial energy of the wavepacket.

Generally, tunneling is exponentially less likely than barrier reflection (for exceptions, see, e.g., Ref. [39]). This follows from the interpretation of tunneling as destructive interference among the Feynman paths underlying quantum dynamics. The introduction of decoherence tends to suppress destructive interference, thereby leading to tunneling enhancement [40]. These dynamics are harvested in Zeno and anti-Zeno quantum control schemes [41].

Figure 1 compares three cases of open and closed dynamics: Figs. 1(a)-(c) show the case where no environment acts on the system ($A_{\pm} = 0$), Figs. 1(d)-(f) show the case where the system is coupled to an environment engineered to enhance tunneling and described by the Lindblad terms (15) with $C = 20$ a.u. and $p_0 = 10^{-4}$ a.u., and Figs. 1(g)-(i) show the case of a coherent free particle [$U(x) = 0$ and $A_{\pm} = 0$]. The plots show Wigner distributions, which are quasiprobability distributions describing the position (horizontal axis) and momentum (vertical axis) of the probe in phase space. The Wigner plots shown in Figs. 1(a)-(f) depict the probe as it approaches the potential barrier, interacts with the barrier, and is either reflected from the barrier [no environment, Figs. 1(a)-(c)] or transmitted through the barrier [engineered environment, Figs. 1(d)-(f)]. The Wigner plots shown in Figs. 1(g)-(i) are provided for comparison and show that the combined effect of the barrier and the environment on the probe is very similar to the case where there is neither a barrier nor an environment, i.e. the case of a coherent free particle. Note that the parameters $C = 20$ a.u. and $p_0 = 10^{-4}$ a.u. were deliberately chosen such that the inequality (13) is satisfied and the probe acts as though it were a coherent free particle. For these parameters, the engineered environment enhances the tunneling rates by three orders of magnitude where the tunneling probability is defined to be the probability that the probe is located to the right of the potential barrier at the conclusion of the simulation.

Figure 2 shows the expectation value of the total energy, $\langle H \rangle$, for the simulations depicted in Fig. 1. The environmental coupling causes $\langle H \rangle$ to first increase as the particle approaches the potential barrier, and then decreases after the particle has tunneled through the potential barrier. In particular, $\langle H \rangle$ does not increase monotonically as a function of time, as would be the case if the environment was simply providing thermal excitation.

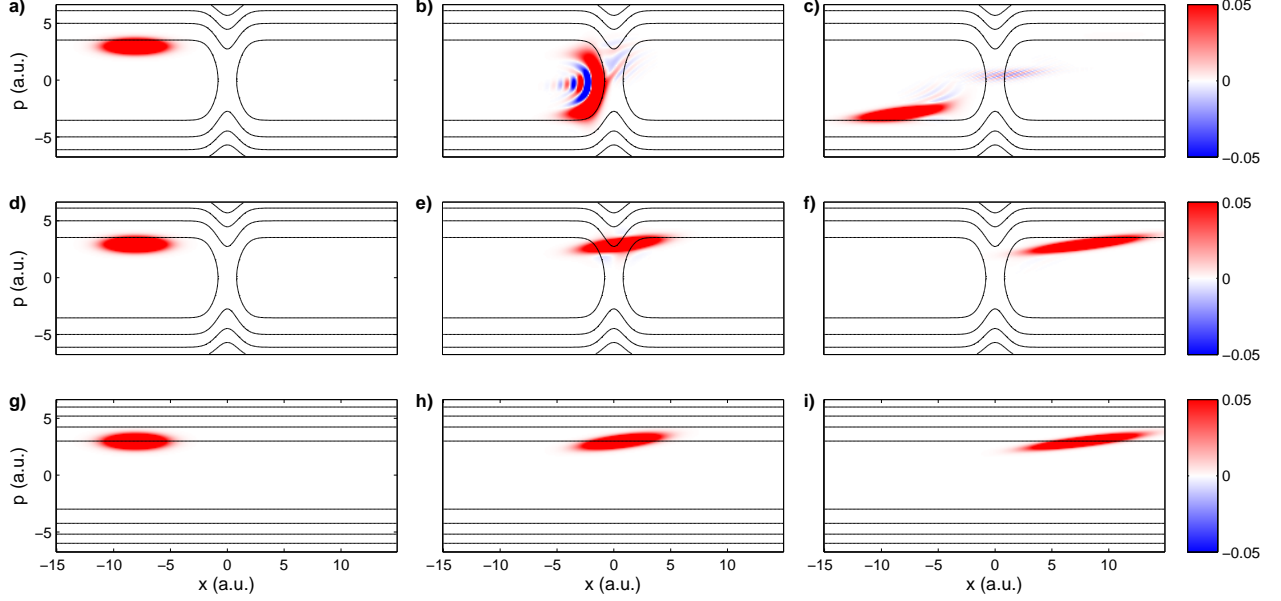


FIG. 1. Wigner function plots for three cases of open and closed dynamics. Plots (a)-(c) depict the closed system: (a) at time = 0 a.u. as the wavepacket approaches the potential barrier, (b) at time = 5600 a.u. as the wavepacket interacts with the potential barrier, and (c) at time = 10000 a.u. after the wavepacket is predominantly reflected from the potential barrier. Plots (d)-(f) depict the open system (3) coupled to an environment described by the Lindblad terms (15): (d) at time = 0 as the wavepacket approaches the potential barrier, (e) at time = 5600 a.u. as the wavepacket interacts with the potential barrier, and (f) at time = 10000 a.u. after the wavepacket predominantly tunnels through the potential barrier. The black lines depict level sets of the Hamiltonian (4) and (19). Plots (g)-(i) depict a coherent free particle (i.e., no barrier and no environment) at the corresponding times and are provided for comparison.

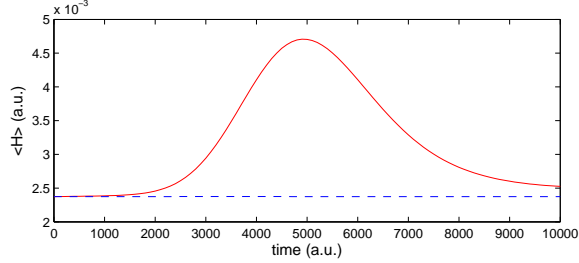


FIG. 2. The expected value of the Hamiltonian for the closed system (blue dashed), and coupled to an environment described by the Lindblad terms (15), (red solid).

Figure 3 compares the tunneling probability and purity for different values of C and p_0 . Consider the energy of each incident electron which, under assumption (13), is equal to $p_0^2/(2m_e)$. Then, the average incident energy per unit time is $\tilde{\sigma} j p_0^2/(2m_e) = (C p_0)^2/(2m_e \hbar)$. The flat regions of the curves correspond to the thermodynamic limit, where there are many collisions per unit time $[(C p_0)^2/(2m_e \hbar) \gg p_0^2/(2m_e)]$ and the effect of each individual collision is negligible. In this regime the total effect of multiple collisions can be represented as an effective

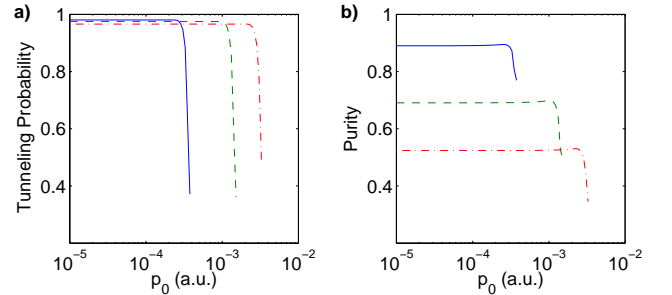


FIG. 3. The tunneling probability (a) and purity (b) for the open system with $C p_0 = 5 \times 10^{-4}$ (blue solid), $C p_0 = 10 \times 10^{-4}$ (green dashed), $C p_0 = 15 \times 10^{-4}$ (red dash-dot).

tive pressure on the probe. Hence, the dynamics of the probe are determined by the total energy of the incident electrons [which is proportional to $(C p_0)^2$], rather than by the number of collisions. Conversely, the sharp drops correspond to the shot noise limit $[C^2/\hbar \sim 1]$, where there are few collisions per unit time, but the effect of each collision is strong. This leads to rapid decoherence, which explains the reduction in tunneling rates and pu-

rity seen in Fig. 3.

Outlook. Historically, noise sources have generally been interpreted as detrimental, and various methods exist for attenuating or decoupling interactions between noise sources and system properties of interest. Physicists and engineers are increasingly looking for new ways to manipulate quantum systems. Hence, dissipative environments are now being viewed in a new way, as a possible resource to be exploited.

We formulate a Lindblad model for quantum statistical forces. Furthermore, we provide an example of how quantum tunneling rates can be enhanced by three orders of magnitude using a dissipative environment that exerts a statistical force opposing the potential barrier. This example encompasses both the thermodynamic and shot noise limits. Utilizing the paradigm of operational dynamic modeling, the given example provides a systematic, general approach for designing dissipative environments. This formalism offers a useful alternative to ad hoc design of dissipative environments. The proposed scheme can be interpreted as a type of open loop control, where the control signal is implemented as a statistical force rather than a potential force. Classical statistical forces exhibit interesting properties such as non-additivity and a non-universal force amplitude. Hence, quantum statistical forces may offer novel control resources for quantum dynamical systems, control resources that are not available through potential interactions.

Acknowledgments. S.L.V. was supported by the Australian Research Council (DP130104510). D.I.B., R.C., H.A.R. respectively acknowledge financial support from NSF CHE 1058644, DOE DE-FG02-02-ER-15344 and ARO-MURI W911NF-11-1-0268. D.I.B. is also supported by 2016 AFOSR Young Investigator Research Program.

[1] A. Aminov, Y. Kafri, and M. Kardar, arXiv:1501.01006 (2015).
 [2] R. M. Neumann, American Journal of Physics **48**, 354 (1980).
 [3] U. Basu, C. Maes, and K. Netočný, Phys. Rev. Lett. **114**, 250601 (2015).
 [4] J. Poyatos, J. Cirac, and P. Zoller, Phys. Rev. Lett. **77**, 4728 (1996).
 [5] F. Verstraete, M. M. Wolf, and J. I. Cirac, Nature Physics **5**, 633 (2009).
 [6] S. Fedortchenko, A. Keller, T. Coudreau, and P. Milman, Phys. Rev. A **90**, 042103 (2014).
 [7] G. Kurizki, E. Shahmoon, and A. Zwick, Physica Scripta **90**, 128002 (2015).
 [8] D. Kienzler, H.-Y. Lo, B. Keitch, L. de Clercq, F. Leupold, F. Lindenfesler, M. Marinelli, V. Negnevitsky, and J. Home, Science **347**, 53 (2015).
 [9] Y. Pan, V. Ugrinovskii, and M. R. James,

Automatica **65**, 147 (2016).
 [10] P. Rouchon, arXiv:1407.7810 (2014).
 [11] A. Metelmann and A. Clerk, Phys. Rev. Lett. **112**, 133904 (2014).
 [12] A. Metelmann and A. A. Clerk, Phys. Rev. X **5**, 021025 (2015).
 [13] A. Miranowicz, J. Bajer, M. Paprzycka, Y.-x. Liu, A. M. Zagoskin, and F. Nori, Phys. Rev. A **90**, 033831 (2014).
 [14] D. V. Zhdanov and T. Seideman, arXiv:1508.04481 (2015).
 [15] V. V. Albert, S. Krastanov, C. Shen, R.-B. Liu, R. J. Schoelkopf, M. Mirrahimi, M. H. Devoret, and L. Jiang, arXiv:1503.00194 (2015).
 [16] J. Cheng, W.-Z. Zhang, L. Zhou, and W. Zhang, arXiv:1511.01267 (2015).
 [17] Y. Liu, S. Shankar, N. Ofek, M. Hatridge, A. Narla, K. Sliwa, L. Frunzio, R. J. Schoelkopf, and M. H. Devoret, arXiv:1509.00860 (2015).
 [18] S. Zippilli, J. Li, and D. Vitali, Phys. Rev. A **92**, 032319 (2015).
 [19] C.-J. Yang, J.-H. An, W. Yang, and Y. Li, Phys. Rev. A **92**, 062311 (2015).
 [20] I. M. Mirza, Journal of Modern Optics, **1** (2015).
 [21] C. Arenz, C. Cormick, D. Vitali, and G. Morigi, Journal of Physics B: Atomic, Molecular and Optical Physics **46**, 224001 (2013).
 [22] A. Kronwald, F. Marquardt, and A. A. Clerk, Phys. Rev. A **88**, 063833 (2013).
 [23] M. J. Woolley and A. A. Clerk, Phys. Rev. A **89**, 063805 (2014).
 [24] F. Qassemi, A. L. Grimsmo, B. Reulet, and A. Blais, arXiv:1507.00322 (2015).
 [25] K. Koga and N. Yamamoto, Phys. Rev. A **85**, 022103 (2012).
 [26] E. T. Holland, B. Vlastakis, R. W. Heeres, M. J. Reagor, U. Vool, Z. Leghtas, L. Frunzio, G. Kirchmair, M. H. Devoret, M. Mirrahimi, and R. J. Schoelkopf, Phys. Rev. Lett. **115**, 180501 (2015).
 [27] M. Asjad and D. Vitali, Journal of Physics B: Atomic, Molecular and Optical Physics **47**, 042001 (2014).
 [28] I. Chestnov, S. Demirchyan, S. Arakelian, A. Alodjants, Y. Rubo, and A. Kavokin, arXiv:1503.07351 (2015).
 [29] A. O. Caldeira and A. J. Leggett, Physica A **121**, 587 (1983).
 [30] C. Somma, K. Reimann, C. Flytzanis, T. Elsaesser, and M. Woerner, Phys. Rev. Lett. **112**, 146602 (2014).
 [31] W. Kuehn, P. Gaal, K. Reimann, M. Woerner, T. Elsaesser, and R. Hey, Phys. Rev. B **82**, 075204 (2010).
 [32] E. Verlinde, Journal of High Energy Physics **2011**, 1 (2011).
 [33] D. I. Bondar, R. Cabrera, R. R. Lompay, M. Y. Ivanov, and H. A. Rabitz, Phys. Rev. Lett. **109**, 190403 (2012).
 [34] D. I. Bondar, R. Cabrera, A. Campos, S. Mukamel, and H. A. Rabitz, J. Phys. Chem. Lett. **7**, 1632 (2016).
 [35] T. Curtright, D. Fairlie, and C. Zachos, Phys. Rev. D **58**, 025002 (1998).
 [36] T. L. Curtright and C. K. Zachos, Asia Pacific Physics Newsletter **01**, 37 (2012).
 [37] T. Curtright, D. B. Fairlie, and C. K. Zachos, *A Concise Treatise on Quantum Mechanics in Phase Space* (World Scientific, 2013).
 [38] R. Cabrera, D. I. Bondar, K. Jacobs, and H. A. Rabitz, Phys. Rev. A **92**, 042122 (2015).
 [39] B. N. Zakharev, V. M. Chabanov, and V. E. Chabanov,

- Submissive quantum mechanics: new status of the theory in inverse problem approach* (Nova Science Pub Inc, 2007).
- [40] Y. Japha and G. Kurizki, Phys. Rev. Lett. **77**, 2909 (1996).
- [41] A. Barone, G. Kurizki, and A. G. Kofman, Phys. Rev. Lett. **92**, 200403 (2004).